

Influence of dephasing process on the quantum Hall effect and the spin Hall effect

Yanxia Xing¹, Qing-feng Sun^{1,*}, and Jian Wang²

¹*Beijing National Laboratory for Condensed Matter Physics and Institute of Physics,
Chinese Academy of Sciences, Beijing 100080, China*

²*Department of Physics and the center of theoretical and computational physics,
The University of Hong Kong, Hong Kong, China*

We study the influence of the phase relaxation process on Hall resistance and spin Hall current of a mesoscopic two-dimensional (2D) four-terminal Hall cross-bar with or without Rashba spin-orbit interaction (SOI) in a perpendicular uniform magnetic field. We find that the plateaus of the Hall resistance with even number of edge states can survive for very strong phase relaxation when the system size becomes much longer than the phase coherence length. On the other hand, the odd integer Hall resistance plateaus arising from the SOI are easily destroyed by the weak phase relaxation during the competition between the magnetic field and the SOI which delocalize the edge states. In addition, we have also studied the transverse spin Hall current and found that it exhibits resonant behavior whenever the Fermi level crosses the Landau band of the system. The phase relaxation process weakens the resonant spin Hall current and enhances the non-resonant spin Hall current.

PACS numbers: 73.23.-b, 72.25.Dc, 73.43.-f, 71.70.Di

I. INTRODUCTION

When the 2D electron system is subjected to a strong perpendicular magnetic field, the energy spectrum becomes a series of impurity broadened Landau bands with extended state in the center^{1,2} of each Landau band and the localized state at the band edges. This gives rise to the integer quantum Hall effect (IQHE),^{3,4} in which the Hall conductance is quantized and jumps from one quantized value to another when the Fermi energy sweeps through the impurity broadened bands or the extended-states. Experimentally,⁵ the quantized unit of Hall conductance $h/2e^2$ can even be specified in parts per million, which becomes a resistance standard that is insensitive to the particular sample and details of its fabrication, because of the spatial separation in the transport states with the opposite velocity and consequently the incredibly long mean free path in the quantum Hall sample. Since the IQHE is discovered in 1980, it has been extensively studied in the past several decades,^{6,7,8,9,10} and the many characteristics of IQHE has been well understood now.

In addition to the quantum Hall effect, the spin Hall effect (in which the longitudinal electronic field induces the transverse spin current), especially the *intrinsic* spin Hall effect (SHE) has recently been intensively studied. Different from the extrinsic SHE which is due to the spin dependent scattering,¹¹ the intrinsic SHE is originated from spin-orbit interaction (SOI). It was predicted first by Murakami *et.al.*¹² and Sinova *et.al.*¹³ in a Luttinger spin-orbit coupled 3D p-doped semiconductor and a Rashba spin-orbit coupled 2D electron gas, respectively. Subsequently, many related works are focused on intrinsic SHE.^{14,15,16,17,18,19,20,21,22} Sheng *et.al.*¹⁴ investigated the SHE in the mesoscopic 2D junction with Rashba SOI, and found that the SHE can survive in the mesoscopic systems with weak disorder. Xing *et al.*¹⁶ found that the

intrinsic SHE is dominated by the extend states, which is different from the IQHE. Besides, the out-of-plane and in-plane component of transverse spin Hall current was studied in a ballistic 2D finite electron system.^{17,18} On the experimental side, Kato *et al.*²⁰ and Wunderlich *et al.*²¹ have observed the transverse opposite spin accumulations near two edges of their devices when the longitudinal voltage bias is added. In addition, the reversal SHE was observed by measuring an induced transverse voltage in a diffusive metallic conductor when a longitudinal net spin current flows through it.²²

Although the IQHE is insensitive to the particular sample and details of its fabrication, it can be transformed to the insulating regime with the weak magnetic field or strong impurity scattering. In fact, global phase diagram of transitions between the quantum Hall states and the insulator (or localized) state has been studied for the quantum Hall system in the tight-binding model²³ and in 2DEG model.²⁴ A phase diagram for the mesoscopic SHE has also been proposed by Qiao *et al.*¹⁹ These works showed both IQHE and SHE can survive in weak disorders and IQHE is more robust than SHE in resistive impurity scatterers. However, in a realistic sample, there exists both impurities or rigid scatters that maintains the phase coherence and the dynamic scatterers like lattice vibration (photons) and electron-electron interactions that induce the phase-relaxation (PR). Hence it is interesting to ask to what extent the IQHE or SHE can survive in the presence of PR processes?

In this paper, we study influence of the PR processes on the IQHE and SHE based on non-equilibrium Green's function (NEGF). We consider a 2D mesoscopic device which is sketched in the inset of Fig.1(c): The central square ballistic region is connected to the four ideal semi-infinite lead-1,2,3 and 4 with the width W . The whole system, including the central region and the four leads, lies in the x, y -plane. A magnetic field B_z is applied in

the positive z -direction. The PR processes in the central region are phenomenologically simulated by introducing the virtual leads²⁵, through which the electrons lose their phase memory. This method was first introduced by Büttiker in 1986. Moreover, there was another method to mimic the dephasing process by Datta and his co-worker.²⁶ This method provides a NEGF-based phenomenological model that is comparable to the virtual leads method with conceptual and numerical simplicity. In the following we will use the virtual leads method (also known as Büttiker probe model in some references) to mimic the dephasing processes. For the system without SOI, the longitudinal current or conductance J_1 (we have set the bias $V_1 - V_3 = 1$) in the lead-1, transverse Hall voltage $V_H = V_2 - V_4$ and the step-like Hall resistance $\rho_H = V_H/J_1$ are calculated numerically with the aid of Green's function method. The results show that IQHE can survive at strong PR process. In particular, the quantized plateaus of the Hall conductance can be kept well even when the PR process is so strong as to completely relax the transport current. In the presence of the SOI, spin degeneracy is broken and odd integer Hall plateaus emerge. These odd number edge states are easily destroyed by weak PR processes. In addition, we also investigate how the SHE is affected by the PR process. It is found that the spin Hall currents $J_{2/4,s}$ show the resonant behaviors when the filling factor changes from odd to even where the Fermi energy is in line with a branch of the eigen levels of the spin polarized system. Furthermore, PR processes weaken the resonant spin current but enhance non-resonant spin current.

The rest of this paper is organized as follows: In Sec. II, the system Hamiltonian and the theoretical formula for calculating the Hall resistance and other quantities are presented. In Sec. III, we show the numerical results and some discussions. Finally, a brief summary is given in Sec. IV.

II. HAMILTONIAN AND FORMULA

Our system (in the absence of phase relaxation and disorders) can be described by the Hamiltonian $H = (-i\hbar\nabla + e\mathbf{A})^2/2m^* + \alpha(\sigma_x\nabla_y - \sigma_y\nabla_x)$ with e the electron charge, m^* the effective mass, α the strength of the Rashba SOI, and $\sigma_{x,y}$ the Pauli matrix. Generally speaking, there are always impurities or disorders in the realistic system giving rise to rigid scatterings which do not contribute to phase-relaxation process. This type of impurity scattering has been extensively investigated using the model of the on-site white-noise potential V_i (i denotes the lattice site) distributed uniformly from $-D/2$ to $D/2$.^{14,16,19} On the other hand, in the presence of phase-randomizing collisions, such as the dynamic scattering by the lattice vibrations (phonon), the electron-electron scattering, and so on, the transport electron loses the phase memory due to these PR processes. Although a proper treatment of non-coherent transport requires

advanced delicate concepts, the basic issues can be accounted for by introducing the virtual leads²⁵ attached to the site \mathbf{i} to mimic the phase-breaking process occurring at the site \mathbf{i} .²⁵ Then the tunneling electrons can escape from the site \mathbf{i} into the virtual leads where the electrons lose phase memory completely and finally return back to the site \mathbf{i} . We assume that the PR processes occur only in the central region and the leads are treated as the measurement terminal which is ideal and clean.

For the central and four real leads, we introduce the tight-binding representation, and the virtual leads are assumed in the free-electron form and expressed in the k -space, which is not necessary but for simplicity. Then, the Hamiltonian is written in the following form:^{16,19}

$$\begin{aligned} H = & - \sum_{\mathbf{i}} \left[a_{\mathbf{i}}^\dagger (te^{-im\phi}\sigma_0 - iV_R\sigma_y)a_{\mathbf{i}+\delta_x} \right. \\ & \left. + a_{\mathbf{i}}^\dagger (t\sigma_0 + iV_R\sigma_x)a_{\mathbf{i}+\delta_y} + H.c \right] \\ & + \sum_{\mathbf{i}} a_{\mathbf{i}}^\dagger [B_z g_s \mu_B \sigma_z / 2] a_{\mathbf{i}} \\ & + \sum_{\mathbf{i},k} \left[\epsilon_k a_{\mathbf{i}k}^\dagger a_{\mathbf{i}k} + (t_k a_{\mathbf{i}}^\dagger a_{\mathbf{i}k} + H.c) \right] \end{aligned} \quad (1)$$

where the first term describes the nearest neighbor coupling and the Rashba SOI in the central region and real leads, in which, $\mathbf{i} = (\mathbf{i}_x, \mathbf{i}_y)$ describes the site of the 2D region shown in the inset of the Fig.1(c). $a_{\mathbf{i}} = [a_{\mathbf{i},\uparrow}, a_{\mathbf{i},\downarrow}]^T$ is the annihilation operator of electrons on the lattice site \mathbf{i} , and δ_x, δ_y are unit vectors along the x and y directions. $\sigma_{x,y,z}$ are Pauli matrices and σ_0 is a 2×2 unit matrix. $t = \hbar^2/2m^*a^2$ is the nearest neighbor hopping matrix element with the lattice constant a . $\phi = qB_z a^2/\hbar$ is the extra phase unit originated from the vector potential \mathbf{A} and m comes from $\mathbf{i}_y = ma$. In the presence of the magnetic field $\mathbf{B} = (0, 0, B_z)$, we introduce the vector potential $\mathbf{A} = (-B_z y, 0, 0)$ in the Landau Gauge, so that the extra phase ϕ occurs in the form $e^{-im\phi}$ in the x -direction. $V_R = \alpha/2a$ denotes the Rashba SOI strength in the tight-binding representation. In our model, the magnetic field B_z is uniform in the whole system, including the four leads and the center region. While the SOI strength V_R exists only in the longitudinal lead-1,3 and the central region, and V_R is set to zero in the transverse lead-2,4. The second term in Eq.(1) denotes the Zeeman split where B_z , g_s and μ_B are the magnetic field along z -direction, the Landé g factor, and Bohr magneton, respectively. Finally, the last term in Eq.(1) represents the Hamiltonian of the virtual leads (described in the k -space) and their coupling to the central site \mathbf{i} . $a_{\mathbf{i}k} = [a_{\mathbf{i}k,\uparrow}, a_{\mathbf{i}k,\downarrow}]^T$ is the annihilation operator of the electrons in the virtual leads, where \mathbf{i} signs the positions of central region. Every central site is coupled by a virtual lead, so there totally are $N = W \times W$ virtual leads, with N being the site number in the central region and W being the width of the central region.

The charge current in real leads J_r ($r = 1, 2, 3, 4$) and in virtual leads J_v ($v = 1, 2, \dots, N$) can be obtained from

the Landauer-Büttiker formula:²⁷

$$J_p = \frac{e^2}{h} \sum_{q \neq p} T_{pq} (V_p - V_q), \quad (2)$$

where $p, q \in r$ or v , V_p is the bias in the lead- p and $T_{p,q}$ is the transmission coefficient from the lead- q to the lead- p . The transmission coefficient can be calculated from $T_{pq} = \text{Tr}[\mathbf{\Gamma}_p \mathbf{G}^r \mathbf{\Gamma}_q \mathbf{G}^a]$, where the line-width function $\mathbf{\Gamma}_p = i(\Sigma_p^r - \Sigma_p^{r\dagger})$ with Σ_p^r the retarded self-energy and the Green's function $\mathbf{G}^r = [\mathbf{G}^a]^\dagger = \{E_F \mathbf{I} - \mathbf{H}_0 - \sum_p \Sigma_p^r\}^{-1}$ where \mathbf{I} is the unit matrix with the same dimension as that of \mathbf{H}_0 . In addition, in order to investigate the SHE, we also need to calculate the spin Hall current $J_{p,s}$ in the transverse lead-2 and 4 for the system with SOI. Because we have set $V_R = 0$ in lead-2 and 4 so that σ is a good quantum number, the particle current $J_{p\sigma}$ in the lead- p ($p = 2, 4$) with spin index σ ($\sigma = \uparrow$ or \downarrow) can be obtained from the Landauer-Büttiker formula:

$$J_{p\sigma} = \frac{e}{h} \sum_{q \neq p} T_{p\sigma,q} (V_p - V_q). \quad (3)$$

The quantities in Eq.(3) are the same as that in Eq.(2), except that here $T_{p\sigma,q}$ is the transmission coefficient from the lead- q to the lead- p with spin σ , and $T_{p\sigma,q} = \text{Tr}[\mathbf{\Gamma}_{p\sigma} \mathbf{G}^r \mathbf{\Gamma}_q \mathbf{G}^a]$ with $\mathbf{\Gamma}_{p\sigma} = i(\Sigma_{p\sigma}^r - \Sigma_{p\sigma}^{r\dagger})$. After obtaining the particle current $J_{p\sigma}$, the spin current $J_{p,s}$ can be easily obtained as $J_{p,s} = (\hbar/2)[J_{p\uparrow} - J_{p\downarrow}]$.

In our calculation, the external bias is applied in the longitudinal leads-1 and 3 with $V_1 = 0.5$ and $V_3 = -0.5$, thus electrons obtain a velocity v_x along the x -direction. With the perpendicular magnetic field, the tunneling electrons deflect to the transverse direction (y -direction) and generates the charge pile up at the vicinity of the lead-2 and lead-4. It consequently leads to opposite transverse Hall voltage $V_2 = -V_4$ in the lead-2 and lead-4 which is calculated by requiring the boundary condition $J_2 = J_4 = 0$ since the lead-2 and 4 only act as the voltage probes. Furthermore, the electrons can only lose their phase memory by escaping into or coming back from the virtual leads, and do not contribute net current to the virtual leads, so there are N extra boundary conditions $J_v = 0$ with $v = 1, 2, \dots, N$. With the transmission coefficient T_{pq} , the input parameters V_1 and V_3 , and the boundary condition $J_{p=2,4,v} = 0$, we can get the transverse bias $V_{2,4}$ ($V_2 = -V_4$) in the lead-2,4 and the longitudinal current $J_{1,3}$ ($J_1 = -J_3$) in the lead-1,3 using Eq.(2). Consequently the Hall voltage $V_H = V_2 - V_4$ and Hall resistance $\rho_H = V_H/J_1$ are obtained straightforwardly. On the other hand, when investigating the SHE we use the boundary condition $V_2 = V_4 = 0$ instead of $J_2 = J_4 = 0$. Then, the particle current $J_{p,\sigma}$ and consequently the spin current $J_{p,s}$ in the lead-2,4 can also be calculated easily.

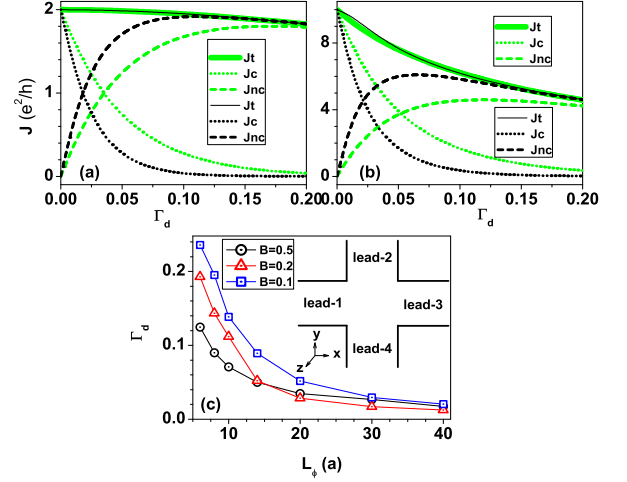


FIG. 1: (Color online) The total current J_t , the coherent component J_c , and the non-coherent component J_{nc} vs. the PR strength Γ_d in the two-terminal non-SOI system for the magnetic field $B = 0.5$ (panel (a)) and $B = 0.1$ (panel (b)) and the system size $W = 20$ (green or gray lines) and $W = 40a$ (black lines). In the Panel (c), the PR strength Γ_d vs. phase coherence length L_ϕ is plotted. Inset of panel (c): Schematic diagram for the mesoscopic four-terminal device.

III. NUMERICAL RESULTS AND DISCUSSION

In the numerical calculation, we fix the Fermi energy²⁸ $E_F = -3t$ which is near the band bottom $-4t$, and take t as energy unit. Here $t = \hbar^2/(2m^*a^2)$ is about $5meV$ while taking $m^* = 0.05m_e$ (the mass of free electron) and the lattice constant $a = 12.5nm$. The size of finite sample W is confined to $W = 40a$ and $20a$. In the presence of magnetic field B_z , there is an extra phase unit $\phi = \frac{q}{\hbar} B a^2$ with the vector potential $\mathbf{A} = (-B_z y, 0, 0)$. When $\phi = 1$, $B = \hbar/(ea^2)$, so we take $\hbar/(ea^2)$ as the unit of the magnetic field B , which corresponds to $B = 4.2T$ and $\mu_B B = 0.05t$. We set Landé g factor $g_s = 2$. Thus Zeeman splitting $\frac{1}{2}g_s\mu_B B = 0.05t$. Moreover, in order to generate the edge states, the cyclotron radius $r_c = v/\omega_c$ must satisfy $r_c < W/2$, then the magnetic field $2/W < B$ is needed. In the SOI system, $V_R = xt$ corresponds to the strength of Rashba SOI $\alpha = 2aV_R \approx 1.25x \times 10^{-10}eVm$ and spin precession length (over which the precessing angle π is generated) $L_{SO} = \pi a/(2x)$. Finally, as a check for our computer program, we have calculated the case in which the magnetic field and the PR process is absent but the spin-orbit interaction is present, the same result as in the Fig.1 of the first reference in Ref.14 can be obtained.

In the experiment, the phase coherent length L_ϕ is a observable parameter and is used to describe all kinds of dephasing processes. Under different experimental conditions, there are different dephasing processes and correspondingly different L_ϕ . So in the following, we will study the relation between the PR strength Γ_d and the phase coherent length L_ϕ . Here we define L_ϕ as the

length, through which the transport electron has 50% probability to lose its phase memory and 50% probability to keep the phase coherence. In the presence of PR processes Γ_d , the current generally consists of both phase coherent part and phase incoherent part. In order to estimate the phase coherence length L_ϕ for a given PR strength Γ_d , we consider a two-terminal structure (decoupled with the lead-2,4), in which the electrons can directly flow from lead-1 to lead-3 or indirectly from lead-1 to lead-3 through virtual leads, the former contributes to the phase coherent current and the latter the incoherent part. Fig.1a and b show the coherent component, the incoherent component, and the total current versus Γ_d for the different system sizes (i.e. the system lengths) $W = 20a$ and $W = 40a$. The total current decreases slightly with the increasing Γ_d , since the edge states carrying the transport electrons are slightly destroyed to the extent proportional to Γ_d . At $\Gamma_d = 0$, the incoherent component is zero and the coherent component is equal to the total current. With the increase of Γ_d , the incoherent component increases and the coherent component decreases. At a certain Γ_d , i.e., at the crossing point of the two curves, the incoherent component is just equal to the coherent component. This means that for this critical Γ_{dc} the system length W is just equal to the phase relaxation length L_ϕ . Therefore the relation between L_ϕ and the PR strength Γ_d can be obtained. Fig.1c shows Γ_d versus L_ϕ for different magnetic fields B . The phase coherence length L_ϕ increases monotonically when Γ_d decreases. Obviously, when $\Gamma_d \rightarrow 0$, $L_\phi \rightarrow \infty$. When Γ_d is not very small (e.g. $\Gamma_d > 0.05t$), the bigger the magnetic field B , the longer L_ϕ is. This is because for the stronger B the edge states are more robust against the PR process. In particular, for the given system size $W = 40a$ and $20a$ used in our following calculation, the critical $\Gamma_{dc} \approx 0.02$ and 0.05 , respectively, beyond which the phase coherence length is smaller than the system size.

A. the IQHE

In this subsection, we study the influence of the PR processes on the IQHE. Firstly, we consider the system without Rashba SOI. In the absence of PR processes ($\Gamma_d = 0$), all of the electrons are carried by the edge states, the electrons traverse clockwise along the sample edge due to the Lorentz force $qv \times B$ (here $B = B_z$ is along the positive z -direction), and the only nonzero matrix elements of the transmission coefficient matrix T are T_{21}, T_{32}, T_{43} and T_{14} with integer values. When PR processes exist ($\Gamma_d \neq 0$), the edge state is partially destroyed. As a result, the elements T_{21}, T_{32}, T_{43} and T_{14} of the transmission coefficients, which denote the edge states, deviate from integer values, and the other elements such as T_{12} become nonzero. In Fig.2, the current J_1 in the lead-1, the transverse Hall voltage V_H and Hall resistivity ρ_H or $1/\rho_H$ versus magnetic field B or $1/B$ are plotted for the different Γ_d . From Fig.2, we can see when

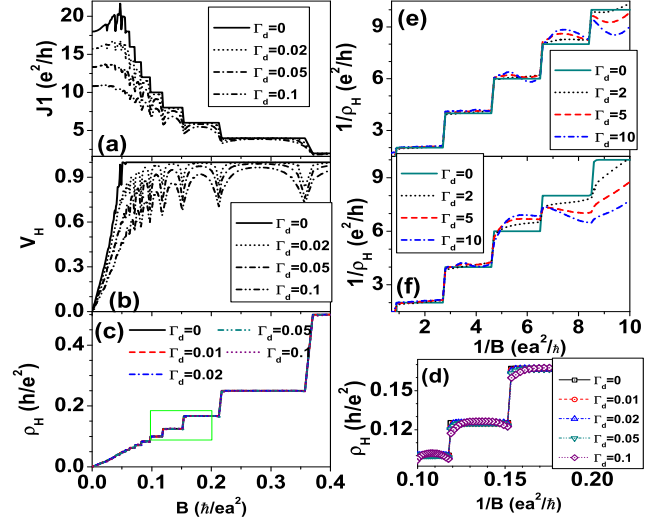


FIG. 2: (Color online) Panel (a)-(c): the current in the lead-1 J_1 , the transverse Hall voltage V_H and Hall resistivity ρ_H vs. magnetic field B for the different PR strength Γ_d , with $V_R = 0$ and $W = 40a$. Panel (d) magnifies the marked region in the panel (c). Inverse of Hall resistivity $1/\rho_H$ vs. the inverse of the magnetic field $1/B$ in the non-SOI system ($V_R = 0$) for the different system size $W = 40a$ (panel (e)) and $W = 20a$ (panel (f)).

the magnetic field ($B < 0.05$) is too small to form edge states, J_1 changes slowly for the variable B and decreases rapidly with Γ_d , the Hall voltage V_H and Hall resistance ρ_H increase linearly with B , which is in agreement with the results of semiclassical Drude model. In the following, we focus on the high fields B case, i.e., B is large enough to separate the flows with the opposite velocity,²⁹ and the system is in the quantum Hall regime. When $\Gamma_d = 0$, the Hall voltage $V_H = V_2 - V_4 = 1$, J_1 and consequently ρ_H exhibit plateaus. This can be understood using the well known picture of Landau level (LL) and the edge state³⁰. In the presence of PR process ($\Gamma_d \neq 0$), J_1 seriously deviates from the even integer plateaus and V_H is no longer a constant. However ρ_H hardly changes and still keeps plateaus even when Γ_d is much bigger than the critical value Γ_{dc} (see Fig.2c and d). This means that although the system is in strong PR regime, the IQHE can survive and is rather robust against the PR processes. From Fig.2(d), we can see that the plateaus are first destroyed at the band edges for large Γ_d . This is because at the band edges of plateaus, E_F is closer to LLs than at the band centers of plateaus. As a result, the electrons are easier to be relaxed to LLs leading to a smaller ρ_H . In Fig.2e and f, we plot $1/\rho_H$ versus $1/B$ for very large Γ_d . The results show that it is more difficult to destroy the plateau at larger magnetic field B or larger sample size. So those plateaus can survive at a bigger Γ_d , i.e., they have stronger ability to resist the PR processes. This is because the energy spacing ΔE between the nearest LLs is larger for the larger magnetic field B , and the edge

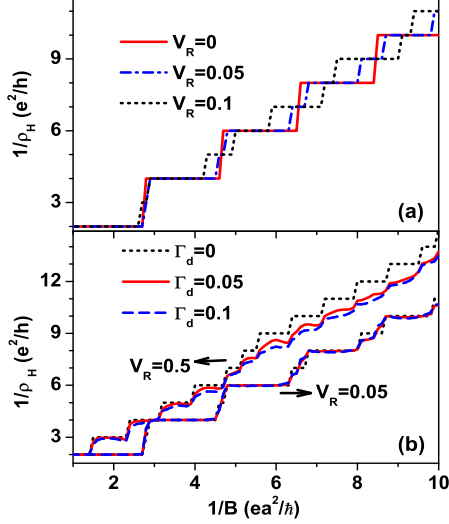


FIG. 3: (Color online) Panel (a): inverse of Hall resistivity $1/\rho_H$ vs. the inverse of magnetic field $1/B$ for the different Rashba SOI strength V_R at $\Gamma_d = 0$. Panel (b): $1/\rho_H$ vs. $1/B$ with $V_R = 0.05t$ and $0.5t$ for different Γ_d . The system size $W = 40a$.

states carrying the opposite current are separated at a larger distance for the larger sample. In particular, the first plateau at $1/B < 3$ can keep well even when Γ_d reaches 10 which is two orders of magnitude larger than the critical value $\Gamma_{dc} = 0.02$ or 0.05 .

Next, we study the system with Rashba SOI V_R . In Fig.3a, $1/\rho_H$ versus $1/B$ for different V_R in the absence of PR processes ($\Gamma_d = 0$) is plotted. It is interesting that although the SOI induces the extended states,¹⁶ $1/\rho_H$ is still quantized and the integer quantum plateaus still remain. At $V_R = 0$, there are only even quanta for $1/\rho_H$. However, as long as $V_R \neq 0$, odd quanta emerge because the spin degeneracy is destroyed. The width of the odd plateau is wider for the larger Rashba SOI strength V_R or for the smaller magnetic field B (see Fig.3a). While at the large V_R , the width of the odd plateau can be in same order with, or even wider than, the width of the even plateau.

In the following, let us study the influence of the PR processes on the plateaus of the IQHE with non-zero Rashba SOI ($V_R \neq 0$). Fig.3 shows $1/\rho_H$ versus $1/B$ for different SOI strengths V_R and PR strengths Γ_d . When V_R is small, for example $V_R = 0.05t$, the even plateaus originated from the edge states are still present. The odd plateaus due to SOI, however, are quickly washed out. While for the strong SOI (e.g. $V_R = 0.5t$) case, the SOI that favors the extend states dominates the magnetic field that favors the edge states, both even and odd plateaus are destroyed by the weak PR process. Notice that for the non-SOI ($V_R = 0$) case the even plateaus can be kept at very large Γ_d which can even reach 10 as shown in Fig.2e and f. The fact that the even plateaus in the SOI system are not as robust against the PR processes as

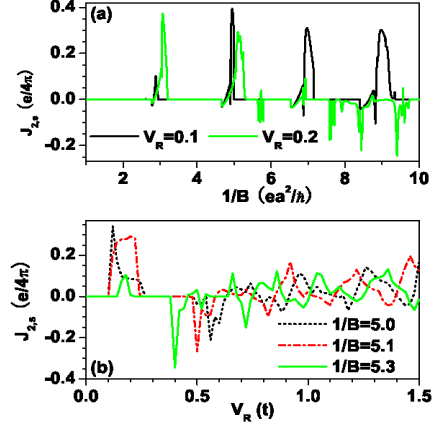


FIG. 4: (Color online) Panel (a): The transverse spin current $J_{2,s}$ vs. inverse of magnetic field $1/B$ for the different Rashba SOI strength V_R . Panel (b): The transverse spin current $J_{2,s}$ vs. the Rashba SOI strength V_R near the resonant peak $1/B \simeq 5.1$ in the panel (a). The other parameters are $\Gamma_d = 0$ and $W = 40a$.

that in the non-SOI system, indicates that the SOI weakens the ability of resisting the PR processes. In fact, the Rashba SOI coefficient α is usually less than $10^{-11} eVm$ for a general 2D electron gas, and the corresponding V_R is less than $0.08t$. With this V_R (e.g. $V_R = 0.05t$), the even plateaus can still survive at $\Gamma_d = 0.1$ which is much larger than the critical value Γ_{dc} .

B. the SHE

In the system with SOI, the SHE occurs, in which a pure and non-dissipating transverse spin current can be generated when a longitudinal electric field or bias is applied. Recently, the SHE has been extensively investigated by a great deal of works as mentioned in the introduction.^{14,15,16,17,18,19,20,21,22} Here we mainly study how the SHE is affected by the magnetic field B , and, in particularly, the PR processes Γ_d . Firstly, the case of $\Gamma_d = 0$ is studied. The transverse spin current $J_{2,s} = -J_{4,s}$ versus $1/B$ for different V_R is plotted in Fig.4(a). An interesting feature is that the spin current $J_{2,s}$ shows a resonant behavior, when the quantized $1/\rho_H$ changes from the odd plateau to the even plateau where the Fermi level is in line with the one of energy eigenvalues of the spin degenerated system. The origin of the resonant spin current will be discussed at last paragraph in this section (see Fig.6). The spin Hall current $J_{2,s}$ is quite large when $1/B$ is near the resonance, but is very small when $1/B$ is far away from it. For $V_R = 0.2$, the resonant positions are about $1/B = 3.1t, 5.1t, \dots$, and for $V_R = 0.1$, they are about at $1/B = 3.0t, 5.0t, 9.0t, 7.0t, \dots$. In

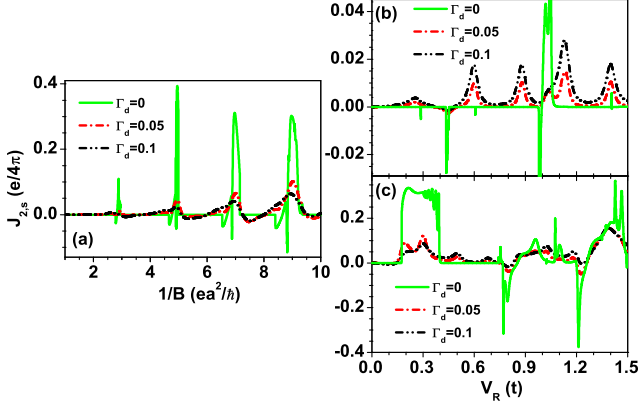


FIG. 5: (Color online) Panel (a): the transverse spin current $J_{2,s}$ vs. inverse of magnetic field $1/B$ for the different PR strength Γ_d at $V_R = 0.1$. Panel (b) and (c): the transverse spin current $J_{2,s}$ vs. the Rashba SOI strength V_R for the different PR strength Γ_d at the off-resonant peak $1/B = 2$ (b) and resonant peak $1/B = 3.1$ (c) in the panel (a). The system size $W = 40a$.

Fig.4(b), we fix the magnetic field $1/B$ at a resonant point ($1/B = 5.1$) and plot $J_{2,s}$ versus V_R . The results show that $J_{2,s}$ is randomly distributed at the large V_R because the extended states are dominant. On the other hand, when $V_R < 0.5t$, $J_{2,s}$ is regular. For $1/B = 5.1$, $J_{2,s}$ is resonant for $V_R = 0.2t$, and there is a stable interval near $V_R = 0.2t$ (see the red dash dotted line in Fig.4b). When $1/B$ deviates from the resonant point 5.1, $J_{2,s}$ is rapidly decay from the resonant V_R (see black dotted line and green solid line in Fig.4b).

In the following, we study the influence of the PR processes Γ_d on the transverse spin current $J_{2,s}$. In Fig.5(a), we plot $J_{2,s}$ vs the magnetic field $1/B$ for different Γ_d . It shows that the PR process Γ_d suppresses the spin current $J_{2,s}$ when $1/B$ is near the resonant points, but enhances $J_{2,s}$ in the off-resonant region. Next, picking up the off-resonant position ($1/B = 2$) and resonant position ($1/B = 3.1$), $J_{2,s}$ versus the SOI strength V_R for different Γ_d are plotted in Fig.5b and c, respectively. Similar to Fig.5(a), the off-resonant spin current is enhanced by the PR processes (see Fig.5b). On the other hand, when the magnetic field is at the resonant point (e.g. $1/B = 3.1$ in Fig.5c), the resonant spin current with V_R from 0.2 to 0.4 is suppressed (see Fig.5c). Moreover, when V_R is very large (e.g. $V_R > 0.5$), the spin current enters the chaotic regime and it depends on the PR processes Γ_d in a random fashion.

Finally, we also study the influence of the Zeeman effect on the SHE. Fig.6(a) and (b) show the spin current $J_{2,s}$ versus the inverse of magnetic field $1/B$ with the SOI strength $V_R = 0$ and $0.1t$, respectively. In each panel, we also plot the corresponding eigenvalues (LLs) of the central scattering region (without leads) versus $1/B$ and assign the resonant positions (see the red dotted lines). When $V_R = 0$, there is only one group of peaks in the

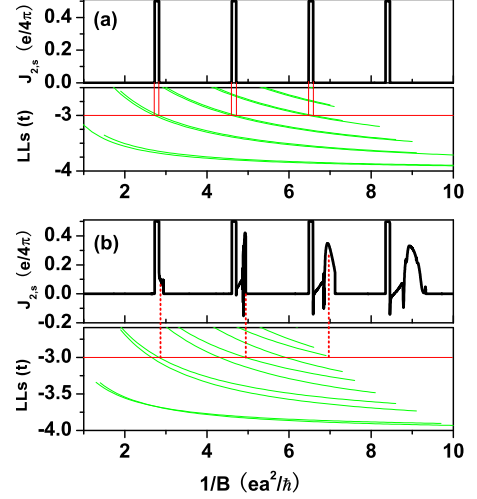


FIG. 6: (color on line) The transverse spin current $J_{2,s}$, the system Landau levels (LLs) vs. inverse of magnetic field $1/B$ while in the presence of the Zeeman effect, with the Rashba SOI strength $V_R = 0$ (a) and $V_R = 0.1t$ (b). The other parameters are $\Gamma_d = 0$ and $W = 40a$. The Fermi level is fixed at $E = -3t$.

curve of $J_{2,s}$ vs $1/B$ due to the Zeeman effect. While for $V_R \neq 0$, the peaks appear in two groups corresponding to the Zeeman peak and resonant peak of spin current. These can be understood as follows. When considering the Zeeman effect, the density of state of electrons for the spin-up and spin-down is different, so LLs are split into the spin-up and spin-down channels. For a given Fermi energy E_F , the number of LLs below E_F for the spin-up and spin-down states can be different. If the number of LLs below E_F are even, the spin current is zero. However, if the number of LLs below E_F is odd, i.e., when E_F is between the split of the LLs, then the spin current is one half and the (Zeeman) peak emerges in the spin current. The positions of peaks are just the positions of LLs (see the red dotted line in fig.6(a)) since the Zeeman split is very small ($0.05t$). On the other hand, in the presence of SOI with $V_R \neq 0$, the LLs for up and down spin channels in the presence of Zeeman term are mixed together and become two new LLs with different spin polarizations. One of LLs is strongly spin polarized while there is no spin polarization for the other LLs. These results are obtained by solving the Schrödinger equation with $V_R \neq 0$. As a result, the resonant spin current emerges when the Fermi level is just in line with the spin-polarized LL (see the red dotted line in Fig.6(b)). So, except for the Zeeman peaks, there are another group of peaks which is originated from different physics in the non-zero SOI system. From Fig.6, we can also see that the intervals of Zeeman peaks are unchanged, while the intervals of the resonant peaks are closer with the decreasing V_R (no shown), which gives an extra evidence that they come from the different physics.

IV. CONCLUSIONS

The effect of PR process Γ_d is investigated in the 2D four-terminal system with or without SOI. Without the SOI, the plateaus of the Hall resistance ρ_H are found to be well kept even when the PR strength Γ_d is very strong (i.e. the phase coherence length is much shorter than the size of system). This means that the IQHE has very strong ability to resist the PR process Γ_d . Furthermore, for the larger sample or the stronger magnetic field, the resistive ability of the PR processes Γ_d is stronger. On the other hand, for the system with SOI, the odd integer plateaus of $1/\rho_H$ are also appear. The odd integer plateaus due to the SOI can be destroyed even for the very weak Γ_d , but the even integer plateaus can still survive in quite strong PR process Γ_d . Next, the SHE, i.e. the transverse spin current, is also studied in the

system with SOI. It is found that the transverse spin current reaches the resonant pole when the Fermi level is just consistent with the one of the two branches of the energy eigenvalues of the system with SOI. The PR process weakens the resonant spin Hall current and enhances the non-resonant spin Hall current. In addition, we also study the properties of system with the Zeeman effect and find there are two group of peaks of the spin current originated from different physics.

ACKNOWLEDGMENTS

We gratefully acknowledge the financial support from NSF-China under Grant Nos. 10525418, 10734110, and 60776060, and a RGC grant from the Government of HK-SAR grant number HKU 7048/06P.

-
- * Electronic address: sunqf@aphy.iphy.ac.cn
- ¹ D. E. Khmel'nitskii, Phys. Lett. **106A**, 182 (1984).
 - ² R. B. Laughlin, Phys. Rev. Lett. **52**, 2304 (1984).
 - ³ For a review, see *The Quantum Hall Effect*, edited by R. E. Prange and S. M. Girvin (Springer-Verlag, New York, 1990).
 - ⁴ K. von Klitzing, G. Dorda, and M. Pepper, Phys. Rev. Lett. **45**, 494 (1980).
 - ⁵ F. Delahaye, D. Deminguez, F. Alerandre, J. P. Andre, J. P. Hirtz, and M. Razeghi, Metrologia, **22**, 103 (1986).
 - ⁶ S. He, X.-C. Xie, S. Das Sarma, and F.-C. Zhang, Phys. Rev. B **43**, 9339 (1990); S. He, X.-C. Xie and F.-C. Zhang, Phys. Rev. Lett. **68**, 3460 (1992).
 - ⁷ V. P. Mineev, Phys. Rev. B **75**, 193309 (2007).
 - ⁸ D. C. Tsui, H. L. Störmer, and A. C. Gossard, Phys. Rev. Lett. **48**, 1559 (1982).
 - ⁹ R. B. Laughlin, Phys. Rev. Lett. **50**, 1395 (1983).
 - ¹⁰ N. Read, Semicond. Sci. Technol. **9**, 1859 (1994). For a review, see *Perspectives in Quantum Hall Effects*, edited by S. DasSarma and A. Pinczuk (Wiley, New York, 1997).
 - ¹¹ J. E. Hirsch, Phys. Rev. Lett. **83**, 1834 (1999). M. I. Dyakonov and V. I. Perel, JETP Lett. **13**, 467 (1971); *ibid.*, Phys. Lett. A **35**, 459 (1971).
 - ¹² S. Murakami, N. Nagaosa and, S. C. Zhang, Science **301**, 1348 (2003); Phys. Rev. B **69**, 235206 (2004).
 - ¹³ J. Sinova, D. Culcer, Q. Niu, N. A. Sinitsyn, T. Jungwirth, and A. H. MacDonald, Phys. Rev. Lett. **92**, 126603 (2004).
 - ¹⁴ L. Sheng, D. N. Sheng, and C. S. Ting, Phys. Rev. Lett. **94**, 016602 (2005); L. Sheng, D. N. Sheng, C. S. Ting, and F. D. Haldane, Phys. Rev. Lett. **95**, 136602 (2005).
 - ¹⁵ S.-Q. Shen Shen, M. Ma, X. C Xie, and F. C. Zhang, Phys. Rev. Lett. **92**, 256603 (2004); S.-Q. Shen, Y.-J. Bao, M. Ma, X. C. Xie, and F. C. Zhang, Phys. Rev. B **71**, 155316 (2005); Y.-J. Bao, H.-B. Zhuang, S.-Q. Shen, and F.-C. Zhang, Phys. Rev. B **72**, 245323 (2005).
 - ¹⁶ Y. Xing, Q.-F. Sun, and J. Wang, Phys. Rev. B **73**, 205339 (2006).
 - ¹⁷ B. K. Nikolić, S. Souma, L. p. Zâbo, and J. Sinova, Phys. Rev. Lett. **95**, 046601 (2005).
 - ¹⁸ Y. Xing, Q.-F. Sun, and J. Wang, Phys. Rev. B **75**, 075324 (2007).
 - ¹⁹ Z. Qiao, J. Wang, and H. Guo, Phys. Rev. Lett. **98**, 196402 (2007); W. Ren, Z. Qiao, J. Wang, Q.-F. Sun, and H. Guo, Phys. Rev. Lett. **97**, 066603 (2006).
 - ²⁰ Y. K. Kato, R. C. Myers, A. C. Gossard, and D. D. Awschalom, Science **306**, 1910 (2004); V. Sih, R. C. Myers, Y. K. Kato, W. H. Lau, A. C. Gossard, and D. D. Awschalom, Nature Phys. **1**, 31 (2005); V. Sih, W. H. Lau, R. C. Myers, V. R. Horowitz, A. C. Gossard, and D. D. Awschalom, Phys. Rev. Lett. **97**, 096605 (2006).
 - ²¹ J. Wunderlich, B. Kaestner, J. Sinova, and T. Jungwirth, Phys. Rev. Lett., **94**, 047204 (2005).
 - ²² S. O. Valenzuela and M. Tinkham, Nature (London) **442**, 176 (2006).
 - ²³ D. Z. Liu, X.-C. Xie, and Q. Niu, Phys. Rev. Lett. **76**, 975 (1996); X.-C. Xie, D. Z. Liu, B. Sundaram, and Q. Niu, Phys. Rev. B **54**, 4966 (1996);
 - ²⁴ S. Kivelson, D.-H. Lee, and S. C. Zhang, Phys. Rev. B **48**, 2223 (1992).
 - ²⁵ M. Büttiker, Phys. Rev. Lett. **57**, 1761 (1986); M. Büttiker, IBM J. Res. Dev. **32**, 317 (1988).
 - ²⁶ Roksana Golizadeh-Mojarad and Supriyo Datta, Phys. Rev. B **75**, 081301 (2007).
 - ²⁷ Chapter 2 and 3, in *Electronic Transport in Mesoscopic Systems*, edited by S. Datta (Cambridge University Press 1995).
 - ²⁸ In the real system, it is not the Fermi energy E_F but the electron density n_s that is fixed while the change of the magnetic field B . If the system has many impure or PR processes and density of state is not sharp change with the energy, the assumption of fixed the Fermi energy E_F instead of fixed the electron density is reasonable.
 - ²⁹ for the simple picture on IQHE, also see Chapter 4, in *Electronic Transport in Mesoscopic Systems*, edited by S. Datta (Cambridge University Press 1995).
 - ³⁰ R. B. Laughlin, Phys. Rev. B **23**, 5632 (1981). B. I. Halperin, *ibid.* **25**, 2185 (1982).